Fan-Beam Computerized Tomography Simulation

Kutay Ugurlu

Abstract—This project report demonstrates the implementation of Fan Beam Computerized Tomography simulation. The effect of different design parameters including the length of the detector, the number of beams and the angle between consecutive projections is inspected and discussed comparatively in both quantitative and qualitative manner. The work is derived from the previously developed code in Parallel Beam X-Ray Computerized Tomography [6]. The developed software and GUI to run it can be found in github.com/kutay-ugurlu/Fan-Beam-Computerized-Tomography-Simulation

Index Terms—imaging, medical imaging, X-Ray computerized tomography, image reconstruction

I. Introduction

The purpose of this project report is to demonstrate the procedure followed to simulate Fan-Beam Projected X-Ray Computerized Tomography. This project report consists of Theory, Implementation, Results and Discussion sections. The second section introduces the technical background for the CT simulation and the following section illustrates the algorithm using pseudocode snippets. Results and Discussion section presents the comparative results regarding different user-specified parameters with the conclusion and reasons behind them.

A. History

The history of X-Ray Computerized Tomography can be dated back to 1917, when an Austrian mathematician called Johann Radon invented an algorithm, referred to as Radon transform today, on how to calculate line integrals in a two-dimensional section. The idea of computed tomography was developed in 1967 and was first used in a medical setting was in 1971 [2], by Godfrey Hounsfield. The device was tested at James Ambrose's department at Atkinson Morley Hospital in Wimbledon. This first model did not include a computer, instead the waves was written on a magnetic tape of the device EMI Scanner CT1010 in Figure 1. It was in 1973 that commercial CT scanners were available to the public. [5]

Fig. 1: First EMI Scanner [7]

II. Theory

A. X-Ray Attenuation

In X-ray tomography, images are modelled as attenuation coefficient distributions which is a measure of how much X-ray beams are attenuated when they propagate through an object. This problem can be modeled as in Eqn. 1 for an arbitrary object.

$$I_{measured} = I_0 e^{-\iiint\limits_{object} \mu(x,y,z)dxdydz} \quad (1)$$

When the object to be imaged is two dimensional or can be reduced to a two dimensional slice, Eqn 1 reduces to Eqn 2:

$$I_{measured} = I_0 e^{-\iint\limits_{slice} \mu(x,y)dxdy} \quad (2)$$

B. Radon Transform

Radon Transform computes the line integrals along the objects to obtain projections along an arbitrary angle θ for an arbitrary beam t, using the formula given in Eqn. 3.

$$p_\theta(t) = \iint\limits_{-\infty}^{\infty} \mu(x,y)\delta(xcos(\theta) + ysin(\theta) - t)dxdy \quad (3)$$

This equation models the X-ray beams as parallel lines through the object. In a more practical scenario, the X-ray source is modelled as a point source and beams are projected from source to the object in fan beam shape, due to the equiangular spaced discrete detector locations. This modelling can be achieved by introducing geometric transformation between projection variables.
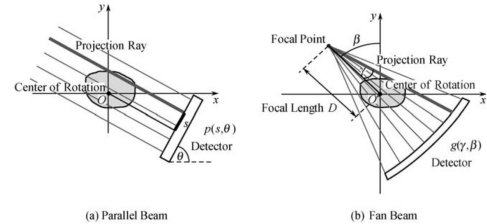

Fig. 2: Parallel Beams and Fan Beams [4]

In Figure 2b, the projection angle with respect to center of rotation is defined as β and the deviation from the center beam that is parallel to the β beam is defined as γ angles. In addition, the source to origin distance is labelled as D, resulting in source to detector distance of $2D$.

With source to detector distance redefined as D and the remaining quantities defined as above, one could transform the equation in 3 to 6 using Eqn. 4 and 5.

$$t = D \cdot sin(\gamma) \tag{4}$$

$$\theta = \beta + \gamma \tag{5}$$

$$p_\beta(\gamma) = \iint\limits_{-\infty}^{\infty} \mu(x,y)\delta(xcos(\theta) + ysin(\theta) \tag{6}$$

$$- Dsin(\gamma))d\gamma d\beta$$

C. Fourier Slice Theorem

The Fourier slice theorem states that Fourier transform of a projection vector $S_\theta(\omega) = \mathcal{F}(p_\theta(t))$ is the section of the original image distribution's Fourier transform $\mathcal{F}(\omega, \theta)$ along the slice of angle θ, which is formally described by Eqn. 7 [1].

$$S_\theta(w) = \mathcal{F}(\omega \cos\theta, \omega \sin\theta) \tag{7}$$

D. Back Projection

According to Fourier Slice theorem, as it is formulated in [1], the original image distribution from projections can be obtained as follows:

$$f(x,y) = \int\limits_{0}^{\pi} \left[\int\limits_{-\infty}^{+\infty} S_\theta(\omega)|w|e^{-j2\pi\omega t}d\omega \right] d\theta \tag{8}$$

The term $|w|$ originates from the Jacobian of the coordinate transformation between Cartesian Space and Polar frequency variables.

$$f(x,y) = \int\limits_{-\infty}^{+\infty}\int\limits_{-\infty}^{+\infty} \mathcal{F}(u,v)e^{-j2\pi(ux+vy)}dudv \tag{9}$$

$$u = \omega \cos\theta \tag{10}$$

$$v = \omega \sin\theta \tag{11}$$

$$dudv = \omega d\omega d\theta \tag{12}$$

The factor ω in Eqn. 12 derives from the Jacobian as follows:

$$J = \begin{vmatrix} \frac{\partial u}{\partial \omega} & \frac{\partial v}{\partial \omega} \\ \frac{\partial u}{\partial \theta} & \frac{\partial v}{\partial \theta} \end{vmatrix} = \begin{vmatrix} \cos\theta & \sin\theta \\ -\omega\sin\theta & \omega\cos\theta \end{vmatrix} \tag{13}$$

$$= \omega(\sin^2\theta + \cos^2\theta) = \omega \tag{14}$$

E. Convolution Back Projection

Eqn. 8 tells us that the 1D Fourier transforms of the projection vectors should be weighted, i.e. filtered, with $|w|$ to obtain the perfect reconstruction of the original unknown distribution. From Eqn. 8, one can deduce that the impulse response of the projection system is $\frac{1}{|\omega|}$, i.e., the components representing the high frequencies in the image distribution is attenuated when they are projected and represented in the Fourier space.

To overcome this low-pass effect, the projections should be filtered with the sequence having the frequency distribution $|w|$. The filter having the band-limited characteristics of above-mentioned frequency response is called Ram-Lak filter.
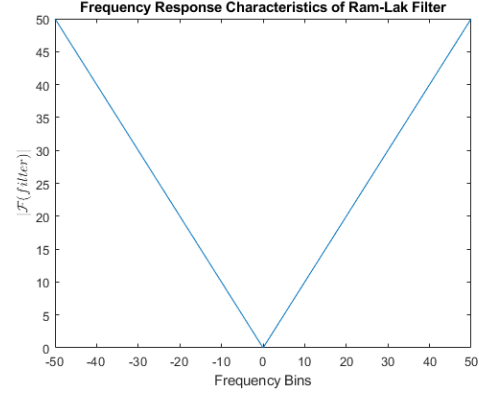

Fig. 3: Ram-Lak filter response

The sharp decrease in the Ram-Lak filter response causes ringing effect in the reconstructed images. To overcome this, the filter can be smoothed out in the higher frequency region with low-pass windows given in Figure 4
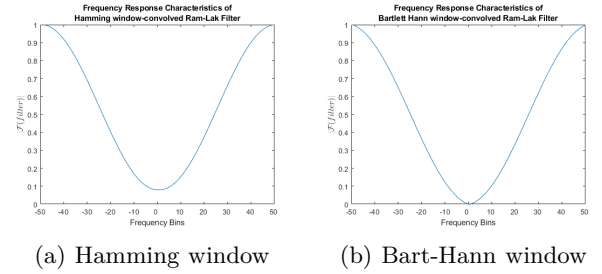

(a) Hamming window

(b) Bart-Hann window

Fig. 4: Smoothing window functions

Then, the resultant filter responses are as follows:

(a) Hamming smoothed Ram-Lak

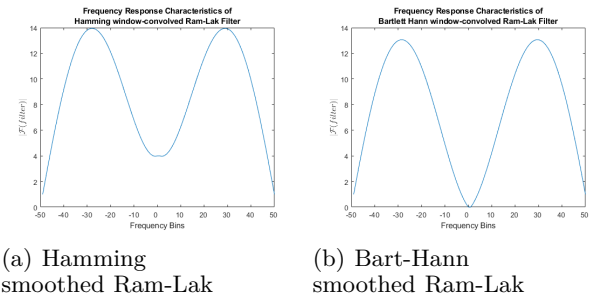(b) Bart-Hann smoothed Ram-Lak

Fig. 5: Ram-Lak filter response smoothed out with window functions

The columns of the projection matrix of size $[\#Rays \times \#ProjectionAngles]$ is convolved with the filters having the responses shown in Figure 5. This operation is called Convolution Back Projection.

III. Implementation

In this section, the computer implementation of the scientific background explained in Section Theory is going to be described.

Algorithm 1 Projection algorithm

---

procedure Projection(I, N_D, L_D, L_{SD})
    Projections = ZEROS
    Form the image Grid $[X(:), Y(:)]$
    for Projection angle β do
        for Fan beam angle γ do
                $\triangleright\ Line = F(x, y, \beta, \gamma)$
            Calculate x intersection
            Calculate y intersection
            Sort $\triangleright$ Regular grid
            Find distance between intersections$\triangleright$ weights
            Find the corresponding pixels
            Calculate projection $\triangleright\ weights \cdot I(pixels)$
            Store in projection matrix
    return Projection matrix

The matrix returned by the procedure defined in Algorithm 1 is used in Algorithm 2 to reconstruct the image.

Algorithm 2 Backprojection algorithm

---

procedure Projection(I, N_D, L_D, L_{SD})
    Projections = ZEROS
    Form the image Grid $[X(:), Y(:)]$
    for Projection angle β do
        for Fan beam angle γ do
                $\triangleright\ Line = F(x, y, \beta, \gamma)$
            Calculate x intersection
            Calculate y intersection
            Sort $\triangleright$ Regular grid
            Find distance between intersections$\triangleright$ weights
            Find the corresponding pixels $\triangleright$ Mid-points
            Sum projections in the pixels $\triangleright\ I(pixel)+ =$
            projection
    return Reconstructed Image

IV. Results

Using the algorithm defined in the Implementation section, all the sample phantoms are reconstructed via Projection and Convolution Back projection algorithm. Figures 6 to 9 are reconstructed utilizing the following projection parameters for angles $0°, 45°, 90°$:

- Number of detectors = 71
- Number of fans = 180
- Source to detector distance = Image size $\times\sqrt{3}$
- Length of the detector = Source to detector distance
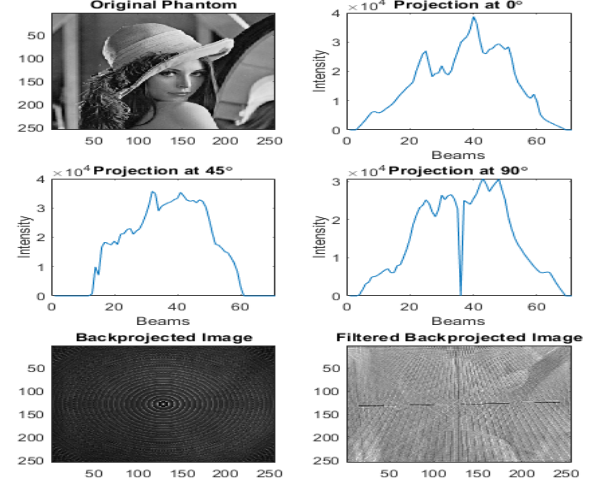

Fig. 6: Projections and reconstructions of Lena phantom
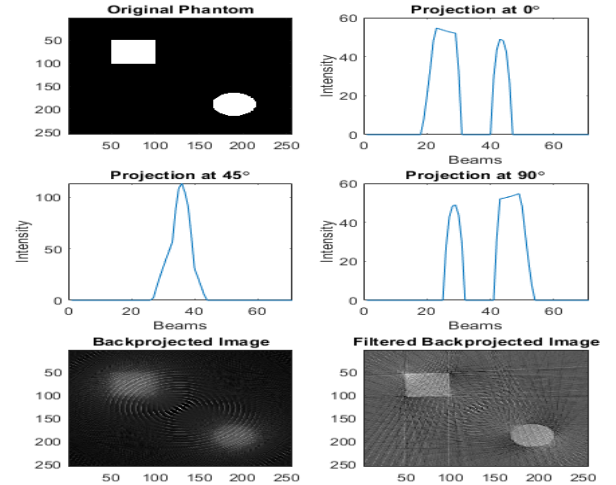

Fig. 7: Projections and reconstructions of Square-Circle phantom
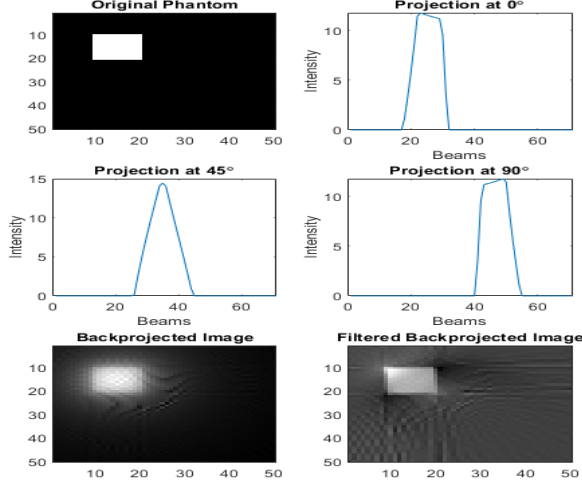
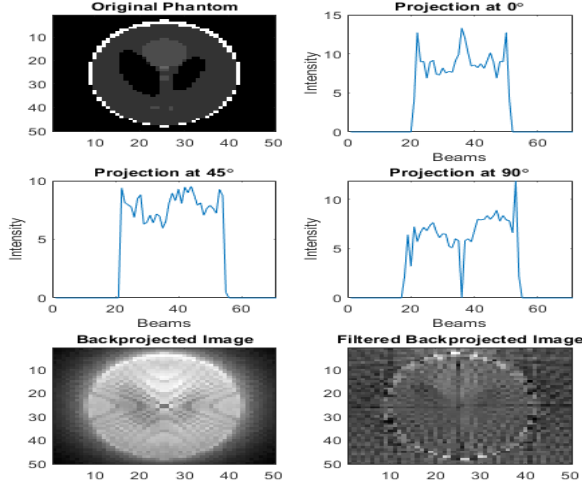Fig. 8: Projections and reconstructions of Square phantom

Fig. 9: Projections and reconstructions of Shepp Logan phantom

In addition, the effect of the parameters such as filter type, projection angle step size and number of detectors are examined using the structural similarity index [3] between the gray intensity pictures of ground truth phantoms and reconstructed images. The results of these experiments are presented in Tables I to III.

Filters \ Phantoms	Shepp Logan	Square	Square Circle
No-filter	0.153	0.100	0.029
Ram-Lak	0.231	0.057	0.032
BartHann	0.246	0.058	0.044
Hamming	0.244	0.058	0.043

TABLE I: SSIM Index for different filter reconstructions

Filters \ Phantoms	50	75	150	300
No-filter	0.015	0.018	0.017	0.035
Ram-Lak	0.019	0.019	0.024	0.039
BartHann	0.027	0.028	0.034	0.048
Hamming	0.026	0.028	0.033	0.048

TABLE II: SSIM Index for different number of beams

Filters \ Phantoms	2	1	0.5	0.25
No-filter	0.022	0.029	0.030	0.030
Ram-Lak	0.025	0.032	0.039	0.043
BartHann	0.028	0.044	0.049	0.048
Hamming	0.027	0.043	0.048	0.048

TABLE III: SSIM Index for different angles

The experiments show that the imaging parameters may affect the reconstructed imaging quality significantly with respect to the case where the parameters are not carefully selected. One example image reconstructed with 0.5° angle step size and 200 detectors can be seen in Figures 10 and 11,
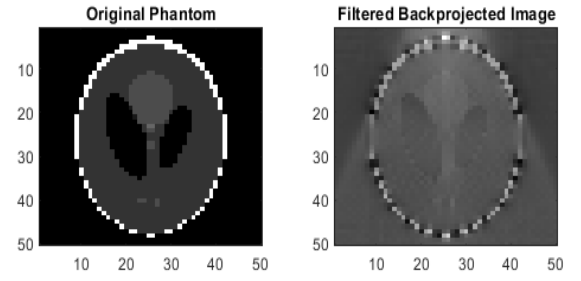

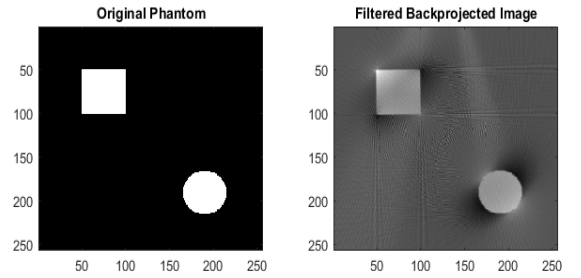Fig. 10: Improved reconstruction of Shepp Logan phantom

Fig. 11: Improved reconstruction of Square Circle phantom

V. Discussion

Some discussion here

References

[1] A. C. Kak and M. Slaney, "Principles of computerized tomographic imaging," in SIAM, 2001, pp. 56–65.
[2] C. Richmond, Sir godfrey hounsfield, 2004.
[3] Z. Wang, A. C. Bovik, H. R. Sheikh, and E. P. Simoncelli, "Image quality assessment: From error visibility to structural similarity," IEEE transactions on image processing, vol. 13, no. 4, pp. 600–612, 2004.

[4] G. L. Zeng, "Image reconstruction: Applications in medical sciences," in Walter de Gruyter GmbH & Co KG, 2017, pp. 51–52.

[5] ISCT, Half a century in ct: How computed tomography has evolved, Jul. 2018. [Online]. Available: https://www.isct.org/computed-tomography-blog/2017/2/10/half-a-century-in-ct-how-computed-tomography-has-evolved#:~:text=Increased%20power%20and%20availability%20of,Laboratories%20using%20x%2Dray%20technology..

[6] K. Ugurlu, "Parallel beam x-ray computerized tomography," 2020.

[7] Emi ct brain scanner: Science museum group collection. [Online]. Available: https://collection.sciencemuseumgroup.org.uk/objects/co134790/emi-ct-brain-scanner-ct-scanner.